

Cobalt Phosphate Based Zeolite Structures with the Edingtonite Framework Topology

Xianhui Bu, Thurman E. Gier, Pingyun Feng, and Galen D. Stucky*

Department of Chemistry, University of California, Santa Barbara, California 93106

Received April 24, 1998. Revised Manuscript Received June 23, 1998

Hydrothermal syntheses and crystal structures of five zeolite edingtonite analogues are presented. For the first time, the edingtonite framework topology is assembled using an amine-assisted synthesis approach with either 1,2-diaminopropane or 1,2-diamino-2-methylpropane. These materials are created in the cobalt phosphate system with a small concentration of trivalent cations (Al^{3+} and Ga^{3+}) incorporated into the framework for the host–guest charge matching. ACP-EDI1 and GCP-EDI1 are monoclinic, whereas ACP-EDI2, ACP-EDI3, and GCP-EDI2 are tetragonal (ACP = aluminum cobalt phosphate; GCP = gallium cobalt phosphate). The difference in lattice symmetries between ACP-EDI1 and ACP-EDI2 (or GCP-EDI1 and GCP-EDI2) is related to the synthesis conditions. All five structures have three-dimensional 8-ring channels along the crystallographic [001], [110], and $[\bar{1}10]$ directions, regardless of the difference in symmetry. Amine molecules are more ordered in the monoclinic phases than in the tetragonal phases, and the orientational disorder of amine molecules persists at a temperature of 150 K.

Introduction

Zeolites are three-dimensional aluminosilicates with open-framework structures. They originally exist as minerals, but their important commercial values have led to extensive academic and industrial research on their syntheses, structures, and various properties.¹ There are now many zeolite structures such as zeolite A that have no natural counterparts, in addition to a variety of zeolite analogue materials with different chemical compositions and framework symmetries.^{2–4} The discovery of a large family of aluminophosphate-based zeolite-type materials in the early 1980s has generated a widespread interest in non-aluminosilicate-based microporous materials.⁵ A similar impressive success has also been achieved in materials containing nontetrahedral metal atoms such as V and Mn.^{6,7}

Our efforts have been on the synthesis of zeolite structures by means of structure direction through host–guest charge matching and hydrogen-bonding-assisted self-assembly in highly charged phosphate systems.^{8–11} We are particularly interested in structures in which the average charge per tetrahedral atom is between 3.75 and 3.5. In such a charge domain, where the framework is highly negatively charged, unusual framework structures with multidimensional

channel systems have been found.^{9,12} These materials may be preferred for some applications, such as gas separation and ion exchange.

One of the challenges facing synthetic chemists is whether all different zeolite topologies found in nature can be assembled using the amine-directed synthesis approach. We have previously reported the first amine-directed synthesis of thomsonite, phillipsite, merlinoite, and rho analogues, which represents a significant step toward achieving that goal.^{8,9,13,14} In this work, we report the first amine-directed synthesis of five structural analogues of a rare zeolite mineral, edingtonite.

Despite the large number of structures that have been found in the AlPO_4 -based system, the edingtonite analogue has until now defied numerous synthetic efforts in either AlPO_4 or substituted AlPO_4 systems.^{15,16} Edingtonite ($\text{Ba}_2\text{Al}_4\text{Si}_6\text{O}_{20} \cdot 8\text{H}_2\text{O}$, space group $P2_12_12$) represents one of three zeolite-type structures (thomsonite and natronite being the other two) that are called fibrous zeolites because their structures comprise a unique chain denoted as the fi chain.¹⁷ So far, only the

- (1) Breck, D. W. *Zeolite Molecular Sieves*; Wiley: New York, 1974.
- (2) Meier, W. M.; Olson, D. H.; Baerlocher, Ch. *Atlas of Zeolite Structure Types*; Elsevier: Amsterdam, 1996.
- (3) Flanigen, E. M. In *Studies in Surface Science and Catalysis*; van Bekkum, H., Flanigen, E. M., Jansen, J. C., Eds.; Elsevier: Amsterdam, 1991; Vol. 58, pp 13–34.
- (4) Chen, J.; Jones, R. H.; Natarajan, S.; Hursthouse, M. B.; Thomas, J. M., *Angew Chem. Int. Ed. Engl.* **1994**, *33*, 639–640.
- (5) Wilson, S. T.; Lok, B. M.; Messina, C. A.; Cannan, T. R.; Flanigen, E. M. *J. Am. Chem. Soc.* **1982**, *104*, 1146–1147.
- (6) Khan, M. I.; Meyer, L. M.; Haushalter, R. C.; Schweitzer, A. L.; Zubieta, J.; Dye, J. L. *Chem. Mater.* **1996**, *8*, 43–53.
- (7) Suib, S. T. *Curr. Opin. Solid State Mater. Sci.* **1998**, *3*, 63–70.

- (8) Feng, P.; Bu, X.; Stucky, G. D. *Nature* **1997**, *388*, 735–741.
- (9) Bu, X.; Feng, P.; Stucky, G. D. *Science* **1997**, *278*, 2271–2272.
- (10) Feng, P.; Bu, X.; Stucky, G. D. *Angew Chem. Int. Ed. Engl.* **1995**, *34*, 1745–1747.
- (11) Bu, X.; Gier, T. E.; Feng, P.; Stucky, G. D. *Microporous Mesoporous Mater.* **1998**, *20*, 371–379.
- (12) Gier, T. E.; Bu, X.; Feng, P.; Stucky, G. D. *Nature* In press.
- (13) Feng, P.; Bu, X.; Stucky, G. D. *Microporous Mesoporous Mater.* In press.
- (14) Feng, P.; Bu, X.; Gier, T. E.; Stucky, G. D. *Microporous Mesoporous Mater.* In press.
- (15) Wilson, S. T.; Flanigen, E. M. In *Zeolite Synthesis*; ACS Symposium Series 398; Ocelli, M. L., Robson, H. E., Ed.; 1989; pp 329–345.
- (16) Kessler, H. In *Comprehensive Supramolecular Chemistry*; Albert, G., Bein, T., Eds.; Pergamon: New York, 1996; Vol. 7, pp 425–464.
- (17) Smith, J. V. *Chem. Rev.* **1988**, *88*, 149–182.

Table 1. A Summary of Crystal Data and Refinement Results

name	ACP-EDI1	GCP-EDI2	ACP-EDI2	ACP-EDI3
formula ^a	(R1) ₂ AlCo ₄ P ₅ O ₂₀	(R1) ₂ GaCo ₄ P ₅ O ₂₀	(R1) ₂ AlCo ₄ P ₅ O ₂₀	(R2) ₂ AlCo ₄ P ₅ O ₂₀
habit	blue plate	blue needle	blue needle	blue prism
size (μm)	133 × 133 × 40	400 × 80 × 80	133 × 67 × 67	53 × 40 × 27
temp (K)	293	150K	293	293
a (Å)	10.0103(5)	9.9937(4)	10.0317(2)	10.0873(3)
b (Å)	9.9896(5)	9.9937(4)	10.0317(2)	10.0873(3)
c (Å)	12.8520(7)	12.8519(7)	12.8837(4)	12.9358(5)
β (deg)	91.113(1)	90	90	90
V (Å ³)	1284.9(1)	1283.57	1296.55(5)	1316.26(8)
Z	2	2	2	2
space group	P2 ₁	P4 ₂ 1c	P4 ₂ 1c	P4 ₂ 1c
2θ _{max} (deg)	50	50	45	45
total data	6646	6313	5076	5044
unique data	3928	1137	852	857
data, I > σ2(I)	3381	726	766	756
parameters	371	84	90	82
R(F) (%)	6.87	5.26	7.89	6.70
R _w (F ²) (%)	17.0	12.7	17.4	12.9
GO _F	1.17	1.13	1.28	1.31

^a R1 = [NH₃CH₂CH(NH₃)CH₃]²⁺; R2 = [NH₃CH₂C(CH₃)₂(NH₃)]²⁺; R(F) = Σ||F_o - |F_c||/Σ|F_o| with F_o > 4.0 σ(F).

crystal structure of aluminosilicate edingtonite has been unambiguously determined from the mineral sample.² One beryllophosphate form (KBePO₄·H₂O) has been reported to have the edingtonite topology on the basis of its powder diffraction data.¹⁸ To our knowledge, no single-crystal study has been done on any synthetic material with the edingtonite-type topology, possibly due to the difficulties in growing large crystals.

Experimental Section

Synthesis. *ACP-EDI1.* ACP-EDI1 was prepared by mixing Co(NO₃)₂ (1.284 g), Al(NO₃)₃ (2.318 g), 2 M H₃PO₄ (2.716 g), and 1,2-diaminopropane (0.89 g) with water (10 mL) in a Teflon pouch. After holding at 150 °C for 1 week at autogenous pressure in an autoclave, the pouch was recovered by standard filtration and drying techniques. Platelike blue crystals were recovered from a colorless solution. No pink or red phases containing nontetrahedral cobalt cations were present, but X-ray powder diffraction data recorded from 3° to 60° (Cu Kα) with a step size of 0.03° and a counting time of 1 s/step on a Scintag PAD X powder diffractometer revealed a few weak unidentified lines, in addition to peaks from ACP-EDI1.

ACP-EDI2. Solution A was prepared by mixing aluminum isopropoxide (100.15 g) with 85% H₃PO₄ (101.74 g) and ethylene glycol (653.00 g), followed by stirring at room temperature for 24 h. In a separate beaker, solution B was made by mixing CoCO₃·xH₂O (13.19 g) with 103.00 g of distilled water, 26.58 g of 85% H₃PO₄, and 32.38 g of solution A. To 19.78 g of solution B was added 1,2-diaminopropane (1.02 g). The mixture was then heated at 180 °C for 4 days in a Teflon-coated steel autoclave. The product was recovered by filtration and washed with deionized water. The blue needlelike crystals were the major product, but a small amount of unidentified pink crystals about 50 μm in size was also present.

ACP-EDI3. To 22.05 g of solution B prepared above was added 1,2-diamino-2-methylpropane (1.37 g) until the pH of the mixture was 6.41. The mixture was then heated at 180 °C for 4 days in a Teflon-coated steel autoclave. The product was recovered by filtration and washed with deionized water. Blue needlelike crystals were the dominant phase, but there was also a small amount of unidentified pink crystals.

GCP-EDI1. A clear solution was made up of 2 M Co(NO₃)₂ (5.136 g, 8 mmol), 2 M HGaCl₄ (1.291 g, 2 mmol), and 2 M H₃PO₄ (4.074 g, 12 mmol) and added to a fluorocarbon film pouch. A solution of 1,2-diaminopropane (2.22 g) in 10 mL of

water was added and the pouch was sealed and heated in an autoclave at 160 °C/100 psi (autogenous, water support fluid) for 30 days. Recovery of the pouch contents via standard ultrasonic/decantation/filtration techniques gave rise to the major product, deep blue crystals, mixed with a small amount of unidentified pink crystalline phases.

GCP-EDI2. This phase was prepared by mixing CoCO₃·xH₂O (0.70 g), 85% H₃PO₄ (1.34 g), Ga(NO₃)₃ (0.34 g), and 1,2-diaminopropane (0.59 g) with ethylene glycol (13.52 g). The mixture was then heated at 180 °C for 4 days in a Teflon-coated steel autoclave. The product was recovered by filtration and washed with deionized water. Blue prismatic crystals were obtained. No unidentified impurity lines could be detected from the X-ray powder diffraction pattern.

Elemental Analysis. Quantitative elemental analyses for ACP-EDI1 and ACP-EDI2 were carried out on a Cameca SX-50 electron probe microanalyzer equipped with five wavelength dispersive (WD) X-ray spectrometers and one energy dispersive (ED) X-ray spectrometer. The instrument was controlled by a SUN workstation, and the analyses for Al, Co, and P were simultaneously performed on three WD spectrometers. The rough surface of ACP-EDI2 and the observed beam damage for ACP-EDI1 might affect the accuracy of the results. The energy dispersive spectrum for GCP-EDI2 showed a small, but distinct, peak for Ga in addition to large Co and P peaks, confirming the substitution of Ga for Co. The following are the calculated analysis values (in mass percent, based on the formula in Table 1) (observed values in parentheses): ACP-EDI1, 3.03 (3.17) Al, 26.5 (24.3) Co, and 17.4 (16.1) P; ACP-EDI2, 3.03 (2.64) Al, 26.5 (23.5) Co, and 17.4 (15.5) P.

Single-Crystal Structure Analysis. Crystal structures of ACP-EDI1 and GCP-EDI2 were refined with both room-temperature and low-temperature data (150 K). GCP-EDI1 was refined only with the low-temperature data. Since the disorder of amine molecules persists at low temperatures and no significant improvements were observed with low-temperature data for either ACP-EDI1 or GCP-EDI2, ACP-EDI2 and ACP-EDI3 were studied only at room temperature. Crystals were glued to thin glass fibers with epoxy resin and mounted on a SMART CCD diffractometer equipped with a normal focus, 2.4 kW sealed tube X-ray source (Mo Kα radiation, λ = 0.71073 Å) operating at 50 kV and 40 mA. The temperature control was achieved with an Oxford Cryostream, which provided a temperature range from 80 to 375 K with a stability of about 0.1 K. About 1.3 hemisphere of intensity data were collected in 1321 frames with ω scans (width of 0.30° and exposure time of 30 s/frame). The empirical absorption corrections were based on the equivalent reflections, and other possible effects, such as absorption by the glass fiber, were simultaneously corrected. The structures were solved by direct

(18) Harvey, G.; Meier, W. M. In *Zeolites: Fact, Figures, Future*; Jacobs, P. A., van Santen, R. A., Eds.; Elsevier: Amsterdam, 1989; pp 411–420.

Table 2. Atomic Coordinates ($\times 10^4$) and Equivalent Isotropic Displacement Parameters ($\text{\AA}^2 \times 10^3$)

atom	x	y	z	$U(\text{eq})^a$	occupancy	atom	x	y	z	$U(\text{eq})^a$	occupancy
ACP-EDI1						ACP-EDI2					
Al(1)	3711(2)	494(2)	5463(2)	28(1)	0.32(1)	Al(1)	-1241(2)	1246(2)	2978(2)	34(1)	0.25
Co(1)	3711(2)	494(2)	5463(2)	28(1)	0.68(1)	Co(1)	-1241(2)	1246(2)	2978(2)	34(1)	0.75
Al(2)	1183(2)	-1991(2)	5497(2)	40(1)	0.17(1)	Co(2)	0	0	0	42(1)	
Co(2)	1183(2)	-1991(2)	5497(2)	40(1)	0.83(1)	P(1)	1480(4)	1410(4)	1799(3)	33(1)	
Al(3)	8711(2)	-4566(2)	10440(2)	30(1)	0.33(1)	P(2)	0	0	5000	41(2)	
Co(3)	8711(2)	-4566(2)	10440(2)	30(1)	0.67(1)	O(1)	2700(12)	2316(12)	1830(16)	95(6)	
Al(4)	3761(2)	-2069(2)	9465(2)	34(1)	0.19(1)	O(2)	824(14)	1520(10)	762(9)	53(3)	
Co(4)	3761(2)	-2069(2)	9465(2)	34(1)	0.81(1)	O(3)	-1909(10)	75(10)	1966(9)	44(3)	
Co(5)	2516(2)	-947(2)	2490(1)	36(1)		O(4)	-1125(12)	481(13)	4329(9)	53(3)	
P(1)	1130(3)	-2377(3)	10620(3)	31(1)		O(5)	546(10)	1858(11)	2664(9)	47(3)	
P(2)	6032(3)	-4450(4)	9254(3)	32(1)		N(1)	1260(15)	3544(17)	4496(14)	62(4)	
P(3)	1011(3)	609(3)	4217(3)	31(1)		C(1)	102(55)	5461(44)	4956(35)	77(14)	
P(4)	2468(3)	-644(4)	7502(2)	31(1)		C(2)	0	5000	6020(24)	132(21)	
P(5)	3928(3)	-2220(3)	4384(3)	31(1)		C(3)	-161(35)	5596(32)	4214(26)	43(9)	
O(1)	2989(11)	-2614(13)	5251(9)	56(3)		ACP-EDI3					
O(2)	3328(13)	-2404(11)	3326(8)	54(3)		Al(1)	-1184(2)	1324(2)	2989(1)	22(1)	0.25
O(3)	5166(12)	-3248(15)	9154(13)	83(5)		Co(1)	-1184(2)	1324(2)	2989(1)	22(1)	0.75
O(4)	1253(11)	-1039(13)	6797(8)	55(3)		Co(2)	0	0	0	26(1)	
O(5)	5594(9)	-5334(11)	10153(8)	46(3)		P(1)	1554(3)	1321(3)	1839(2)	22(1)	
O(6)	1983(10)	1074(11)	5081(8)	46(3)		P(2)	0	0	5000	18(1)	
O(7)	2972(13)	-1855(12)	8098(8)	59(3)		O(1)	2792(9)	2152(9)	1887(9)	52(3)	
O(8)	1043(10)	-1827(14)	1711(8)	52(3)		O(2)	938(9)	1421(8)	761(6)	33(2)	
O(9)	3598(9)	-74(12)	6851(7)	44(3)		O(3)	-1925(9)	123(8)	2034(7)	38(2)	
O(10)	2593(10)	-2804(11)	10452(8)	46(3)		O(4)	-1105(9)	629(8)	4342(6)	31(2)	
O(11)	4365(10)	-766(11)	4509(8)	50(3)		O(5)	584(9)	1815(9)	2647(7)	38(3)	
O(12)	5905(10)	-5242(14)	8254(8)	54(3)		N(1)	1318(15)	3628(15)	4551(11)	63(4)	
O(13)	1704(12)	568(12)	3191(8)	52(3)		C(1)	931(19)	5904(19)	5732(14)	67(5)	
O(14)	2007(12)	460(12)	8224(8)	54(3)		C(2)	-330(25)	5503(25)	4110(19)	30(6)	
O(15)	693(10)	-1328(11)	9824(8)	50(3)		C(3)	0	5000	5062(20)	68(7)	
O(16)	534(10)	-793(12)	4438(8)	49(3)		GCP-EDI2					
O(17)	5170(13)	-3081(14)	4532(14)	91(5)		GA(1)	-1211(2)	1261(2)	2981(1)	31(1)	0.25
O(18)	-97(14)	1589(14)	4105(12)	85(5)		Co(1)	-1211(2)	1261(2)	2981(1)	31(1)	0.75
O(19)	230(12)	-3568(14)	10485(12)	81(4)		Co(2)	0	0	0	29(1)	
O(20)	7468(9)	-3982(13)	9409(9)	55(3)		P(1)	1499(4)	1386(4)	1784(3)	32(1)	
N(11)	1273(13)	2779(19)	6972(14)	74(5)		P(2)	0	0	5000	37(2)	
N(12)	3754(14)	5727(15)	6957(11)	58(4)		O(1)	2722(13)	2224(13)	1732(14)	92(5)	
C(11)	2058(47)	3774(36)	7425(19)	275(36)		O(2)	773(12)	1521(10)	757(7)	49(3)	
C(12)	2777(32)	4638(34)	6671(22)	134(14)		O(3)	-1904(10)	101(9)	1933(8)	45(3)	
C(13)	2288(34)	4412(37)	8515(18)	153(17)		O(4)	-1200(11)	426(12)	4337(8)	52(3)	
N(21)	-3918(16)	387(18)	8021(13)	71(5)		O(5)	581(10)	1857(10)	2642(8)	46(3)	
N(22)	-972(14)	-2074(15)	8011(12)	59(4)		N(1)	1221(18)	3552(17)	4486(14)	76(5)	
C(21)	-3224(25)	-937(31)	7693(22)	180(19)		C(1)	0	5000	6041(28)	89(10)	
C(22)	-1800(19)	-897(26)	8082(30)	136(13)		C(2)	0	5000	4837(78)	241(43)	
C(23)	-2867(51)	-1026(39)	6512(17)	197(24)		C(3)	0	5000	4112(74)	225(36)	

^a $U(\text{eq})$ is defined as one-third of the trace of the orthogonalized U_{ij} tensor.

methods followed by successive difference Fourier methods. All calculations were performed using SHELXTL running on a Silicon Graphics Indy 5000. Final full-matrix refinements were against F^2 and the crystallographic results are summarized in Table 1. Positional coordinates are listed in Table 2, while selected bond distances are given in Table 3.

Results and Discussion

ACP-EDI1 and GCP-EDI1. ACP-EDI1 was prepared under synthesis conditions significantly different from those used in the preparation of many other cobalt phosphate based materials reported earlier.⁸ No organic cosolvent was present, and very different cobalt and aluminum sources (nitrates instead of carbonates and alkoxides) were used. Also noteworthy was the reaction temperature (150 °C), because most cobalt phosphate based zeolite structures we have reported so far were made at a higher temperature (180 °C).⁸ Thus, the successful synthesis of ACP-EDI1 has further expanded the rich synthetic and structural chemistry of the ternary cobalt phosphate system.

ACP-EDI1 has a characteristic pseudotetragonal cell typical for an edingtonite structure. The monoclinic cell

of ACP-EDI1 is unique because all other edingtonite structures have been described in either tetragonal or orthorhombic systems. Such a symmetry reduction might be due to the ordering of organic molecules in ACP-EDI1. The doubling of the c axis (12.85 Å for ACP-EDI1) as compared to the aluminosilicate form (6.5 Å for the mineral edingtonite) is due to the ordered distribution of metal and phosphorus atom sites. The fi chain propagates along the crystallographic c axis and there are 8-ring channels running along the same direction (Figure 1). The fi chains are cross-linked in two mutually perpendicular directions, i.e., crystallographic [110] and $[1\bar{1}0]$ directions (Figure 1). These two directions coincide with two other 8-ring channels (Figure 2). Thus, the framework of ACP-EDI1 consists of a three-dimensional, intersecting, orthogonal channel system.

The structure of edingtonite is very similar to that of thomsonite or natrolite. What distinguishes the edingtonite topology from that of thomsonite and natrolite is that the secondary building unit (denoted as $4=1$)¹⁹ does not change the orientation between adjacent chains (Figure 1), whereas in thomsonite, the $4=1$ units change

Table 3. Selected Bond Lengths (Å)

ACP-EDI1			
Co(1)–O(17)	1.812(12)	Co(1)–O(9)	1.877(10)
Co(1)–O(6)	1.880(10)	Co(1)–O(11)	1.883(11)
Co(2)–O(18)	1.864(13)	Co(2)–O(16)	1.917(11)
Co(2)–O(4)	1.923(11)	Co(2)–O(1)	1.944(12)
Co(3)–O(19)	1.818(11)	Co(3)–O(14)	1.874(10)
Co(3)–O(15)	1.891(12)	Co(3)–O(20)	1.893(10)
Co(4)–O(3)	1.883(12)	Co(4)–O(10)	1.889(11)
Co(4)–O(5)	1.911(11)	Co(4)–O(7)	1.924(10)
Co(5)–O(13)	1.947(12)	Co(5)–O(8)	1.974(11)
Co(5)–O(2)	1.975(10)	Co(5)–O(12)	1.991(11)
P(1)–O(19)	1.500(12)	P(1)–O(8)	1.509(11)
P(1)–O(15)	1.523(10)	P(1)–O(10)	1.545(10)
P(2)–O(3)	1.485(12)	P(2)–O(12)	1.512(11)
P(2)–O(20)	1.521(10)	P(2)–O(5)	1.525(11)
P(3)–O(18)	1.484(12)	P(3)–O(13)	1.503(11)
P(3)–O(16)	1.508(12)	P(3)–O(6)	1.534(10)
P(4)–O(7)	1.514(11)	P(4)–O(14)	1.520(12)
P(4)–O(9)	1.530(10)	P(4)–O(4)	1.554(11)
P(5)–O(2)	1.488(11)	P(5)–O(17)	1.520(12)
P(5)–O(11)	1.524(11)	P(5)–O(1)	1.523(12)
ACP-EDI2			
Co(1)–O(1)	1.808(12)	Co(1)–O(3)	1.878(10)
Co(1)–O(4)	1.907(12)	Co(1)–O(5)	1.938(11)
Co(2)–O(2)	1.993(11)	Co(2)–O(2)	1.993(11)
Co(2)–O(2)	1.993(11)	Co(2)–O(2)	1.993(11)
P(1)–O(2)	1.493(13)	P(1)–O(5)	1.524(12)
P(1)–O(1)	1.525(12)	P(1)–O(3)	1.565(11)
P(2)–O(4)	1.501(12)	P(2)–O(4)	1.501(12)
P(2)–O(4)	1.501(12)	P(2)–O(4)	1.501(12)
ACP-EDI3			
Co(1)–O(1)	1.859(9)	Co(1)–O(3)	1.885(8)
Co(1)–O(4)	1.888(8)	Co(1)–O(5)	1.904(9)
Co(2)–O(2)	1.979(9)	Co(2)–O(2)	1.979(9)
Co(2)–O(2)	1.979(9)	Co(2)–O(2)	1.979(9)
P(1)–O(1)	1.505(9)	P(1)–O(5)	1.515(9)
P(1)–O(3)	1.525(9)	P(1)–O(2)	1.530(9)
P(2)–O(4)	1.539(8)	P(2)–O(4)	1.539(8)
P(2)–O(4)	1.539(8)	P(2)–O(4)	1.539(8)
GCP-EDI2			
Co(1)–O(1)	1.889(12)	Co(1)–O(3)	1.911(9)
Co(1)–O(4)	1.936(10)	Co(1)–O(5)	1.938(10)
Co(2)–O(2)	1.965(10)	Co(2)–O(2)	1.965(10)
Co(2)–O(2)	1.965(10)	Co(2)–O(2)	1.965(10)
P(1)–O(1)	1.484(12)	P(1)–O(5)	1.513(11)
P(1)–O(2)	1.515(11)	P(1)–O(3)	1.553(10)
P(2)–O(4)	1.534(10)	P(2)–O(4)	1.534(10)
P(2)–O(4)	1.534(10)	P(2)–O(4)	1.534(10)

the orientation in one direction, and in natrolite, the 4=1 units change the orientation in both directions.²⁰ Thus, the fibrous chains in edingtonite are cross-linked in the simplest manner.

There are five crystallographically unique metal atom sites in ACP-EDI1 (Figure 3a). The average metal to oxygen distances are 1.863, 1.912, 1.912, 1.869, 1.902, and 1.972 Å, respectively (Table 3). The variation in bond distances is due to the different Co/Al ratio at each site. In amine-templated ternary phosphate zeolite structures, when there are two or more crystallographically unique metal atom sites, the Co/Al ratio is rarely the same throughout all sites.⁸ Since the ideal Al–O or Ga–O bond distance (1.74 Å for Al–O or 1.82 Å for Ga–O) is shorter than the Co–O bond (1.93 Å),²¹ the incorporation of Al³⁺ or Ga³⁺ atoms into the Co²⁺ sites reduces the observed metal to oxygen bond distances.

(19) Meier, W. M.; Olson, D. H. *Atlas of Zeolite Structure Types*; Butterworth-Heinemann: Stoneham, MA, 1992.

(20) Gottardi, G.; Galli, E. *Natural Zeolites*; Springer-Verlag: New York, 1985; pp 6–8.

(21) Shannon, R. D. *Acta Crystallogr.* **1976**, *A32*, 751–767.

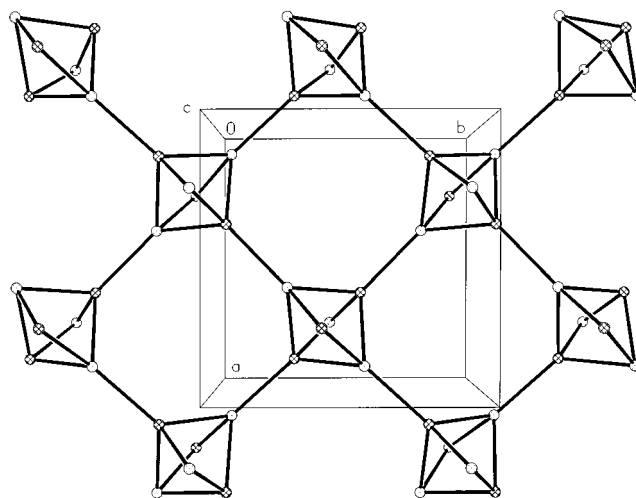


Figure 1. The framework of ACP-EDI1 projected down the crystallographic *c* axis showing 8-ring channels and directions in which fi chains are cross-linked. The crosshatched circles represent metal atom sites.

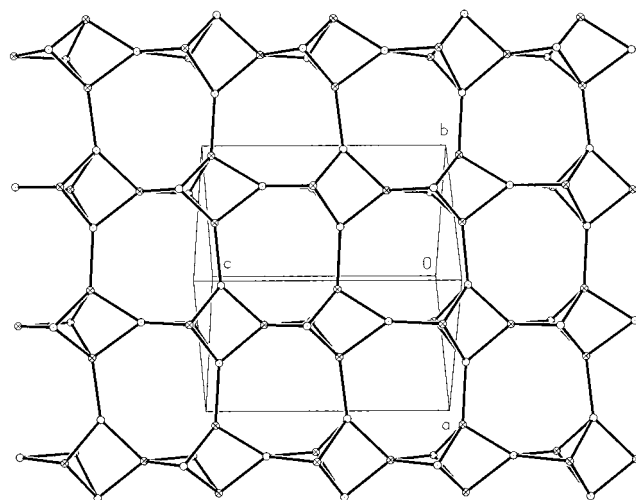


Figure 2. The 8-ring channels along the crystallographic [110] direction in ACP-EDI1. The crosshatched circles represent metal atom sites. The fi chains are shown running along the *c* axis.

The correlation between the Co²⁺ concentration at metal atom sites and metal–oxygen bond distances has been fully discussed before and is very useful in the structural characterization of ternary phosphate structures.⁸ It has been observed that the metal to oxygen bond distance is 1.83 Å when the Co/Al ratio is 1:1.⁸ Thus on the basis of the M–O distances in ACP-EDI1, all metal atom sites are dominated by Co²⁺ cations. In fact, the Co5 site is likely to be a pure Co site, whereas Co1 and Co3 sites have relatively high Al³⁺ substitutions (Table 2).

Even though a large number of cobalt phosphate based zeolite analogues and novel structures have been discovered, the high transition metal concentration in the edingtonite analogues is not common among zeolite structures. Only thomsonite analogues have the same high transition metal concentration as the edingtonite analogues reported here.⁸

There are two unique diprotonated amine molecules in the asymmetric unit of ACP-EDI1 (Figure 3b). While the carbon atoms of these amine molecules have highly

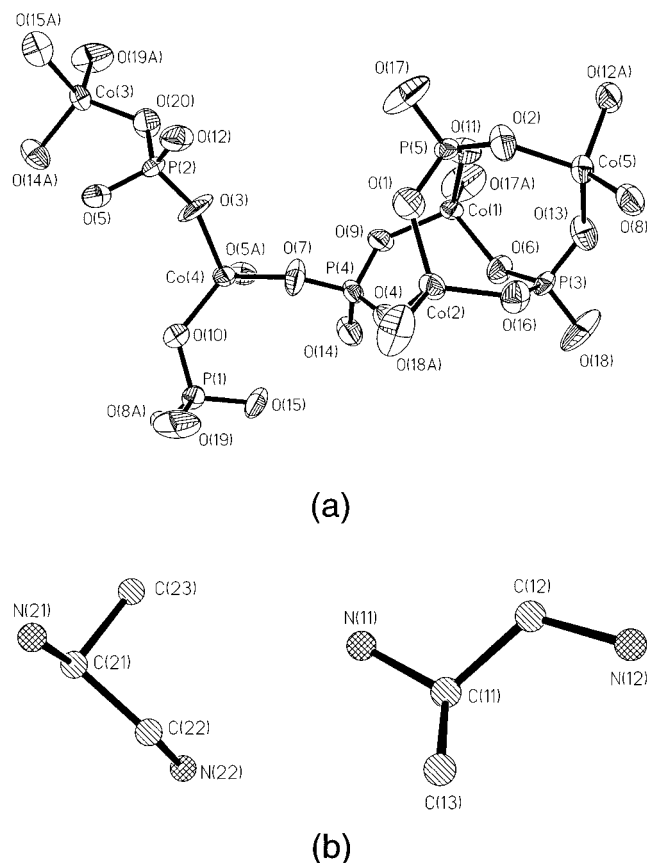


Figure 3. (a) An ORTEP (50%) drawing showing the local coordination environment in ACP-EDI1. Atoms with labels containing "A" are symmetry generated and (b) two independent 1,2-diaminopropane molecules in ACP-EDI1.

anisotropic thermal parameters, all four unique nitrogen atoms are highly ordered. Similar thermal parameters for C and N atoms are also observed at 150 K, suggesting that the large thermal parameters of C atoms are due to the static positional disorder. The strong ordering of nitrogen atoms suggests the presence of N—H...O type hydrogen bonds, which are believed to play an essential role in the self-assembly of the inorganic framework. The observed short N...O distances of less than 3.0 Å support the formation of hydrogen bonds. The shortest N...O distance is 2.842 Å between O1 and N12. It is of interest to point out that while 1,2-diaminopropane templates the formation of the edingtonite topology, two closely related amines, 1,3-diaminopropane and *N*-methylethylenediamine, structure direct the formation of the thomsonite topology.⁸

An understanding of the functions of organic amines is of vital importance in the synthesis of zeolite-type materials. In ACP-EDI1, the different ordering of N and C atoms suggests that amine molecules play a dual role in the cooperative self-assembly of inorganic framework: active and passive. The active role is that amines control the framework formation processes through strong N—H...O interactions. Thus the separation between two NH₃⁺ groups determines the largest possible cage size or pore dimension. In this case, the relatively short separation (only two C atoms) gives rise to 8-ring channels with no apparent cages. In comparison, 1,7-diaminoheptane gives rise to a structure with large cages and large pore sizes.⁹ The passive role comes from the conformational flexibility of amine

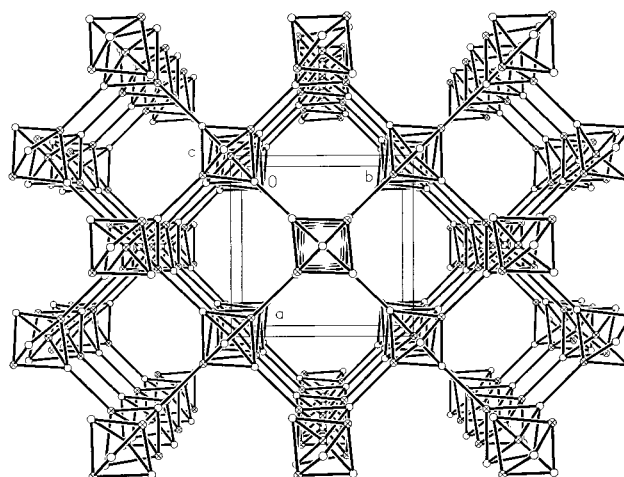


Figure 4. The framework of GCP-EDI2 projected down the crystallographic *c* axis. The crosshatched circles represent metal atom sites.

molecules and their tendency to become orientationally disordered to conform to the symmetry of the inorganic framework. These two roles can both be important in the condensation process of the inorganic species.

Crystals of GCP-EDI1 are large but of poor quality. All crystals have irregular shapes and rough surfaces. The spurious reflections can be detected at the unit cell indexing stage. The unit cell parameters at 150 K refined using 2464 reflections are $a = 10.0343(3)$ Å, $b = 9.9698(2)$ Å, $c = 12.8619(5)$ Å, $\beta = 91.849(2)^\circ$, confirming the edingtonite-type framework topology. The structural refinement is, however, less satisfactory [$R(F) = 16.0\%$] than for the other four edingtonite analogues reported here. Such a high R factor is likely due to the less accurate intensity data resulting from twinning. There is little doubt that GCP-EDI1 is isostructural to ACP-EDI1 and is different from the tetragonal GCP-EDI2 phase described below.

GCP-EDI2. GCP-EDI2 was prepared using ethylene glycol as the only solvent (a small amount of water from Co and P sources was present). The structure of GCP-EDI2 is very similar to that of ACP-EDI1, but GCP-EDI2 has a higher symmetry. Amine molecules are located on the 2-fold axes and are disordered. Data collected at 150 K indicate that the disorder of amines persists at low temperatures. Such an orientational disorder of amine molecules can be attributed to the symmetry mismatch between the inorganic framework and amine molecules.

There are two unique metal atom sites with average M—O distances of 1.918 and 1.965 Å, respectively. Compared to the Al—O bond, the length of the Ga—O bond is closer to that of the Co—O bond. Thus, the incorporation of Ga³⁺ cations into Co²⁺ sites does not lead to a significant shortening of the observed M—O distances in GCP-EDI2. Just like ACP-EDI1, there are three-dimensional 8-ring channels along the crystallographic [001], [110], and $[\bar{1}10]$ directions (Figure 4)

ACP-EDI2 and ACP-EDI3. ACP-EDI2 was synthesized under conditions significantly different from that of ACP-EDI1. ACP-EDI2 was prepared from a partially nonaqueous solvent, and aluminum isopropoxide and hydrated cobalt carbonate were used as Al³⁺ and Co²⁺ sources, respectively. ACP-EDI3 was prepared under

similar conditions but using a different structure-directing agent (1,2-diamino-2-methylpropane). Similar synthesis conditions were previously used in the creation of a large number of cobalt phosphate based materials.⁸ Crystals of ACP-EDI2 and ACP-EDI3 are noticeably smaller than those of ACP-EDI1 and GCP-EDI2 but are large enough for single-crystal diffraction studies. It appears that a limiting factor for the quality of the structure refinement is the disorder of amine molecules, not the size of crystals.

ACP-EDI2 and ACP-EDI3 have the same framework composition and topology as ACP-EDI1 and their lattice symmetries are identical to that of GCP-EDI2. As in GCP-EDI2, there is no problem locating the overall location of amine molecules, but the atomic positions of C and N atoms are not well-defined due to the orientational disorder of the amine molecules. Thus the C and N coordinates given in Table 3 for ACP-EDI2, ACP-EDI3, and GCP-EDI2 are meaningful when they are interpreted as representing the general location of amine molecules. They do not define a specific orientation of an amine molecule.

In conclusion, the success in synthesizing the new edingtonite materials is largely due to the realization of the importance of host–guest charge density matching in the cooperative inorganic–organic self-assembly

processes. The lack of any mineral zeolite analogue in the binary cobalt phosphate system is not because of our inability to find the proper geometrical fit between the inorganic host and organic guest molecules but because of the host–guest charge density mismatch. The introduction of trivalent metals such as Al³⁺ into the cobalt phosphate system, however, provides the flexibility in adjusting the framework charge density by varying the Co/Al ratio. This extra variable (the Co/Al ratio) makes it possible to synthesize many ternary phosphate structures isotypic to aluminosilicate zeolites.

Acknowledgment. This research was supported in part by the National Science Foundation under Grant DMR 95-20971. A Materials Research Laboratory Corning Foundation Fellowship for P.F. is gratefully acknowledged. We thank D. Pierce from the Department of Geological Sciences for help with the electron probe microanalysis.

Supporting Information Available: Crystallographic details for ACP-EDI1, ACP-EDI2, ACP-EDI3, and GCP-EDI2, including anisotropic temperature factors (8 pages). Ordering information is given on any current masthead page.

CM980308D